Available online at www.sciencedirect.com
SCIENCE DIRECT®
Computers and Structures 82 (2004) 639–651
Computers & Structures
www.elsevier.com/locate/compstruc

# Beam element formulation and solution procedure for dynamic progressive collapse analysis

Griengsak Kaewkulchai, Eric B. Williamson *

*Department of Civil Engineering, University of Texas at Austin, Austin, TX 78712-1076, USA*

Received 24 December 2002; accepted 12 December 2003

**Abstract**

A beam element formulation and solution procedure for progressive collapse analysis of planar frame structures is presented. Unlike previous research, the current study addresses the significance of dynamic load redistribution following the failure of one or more elements. The developed beam-column element utilizes a multi-linear, lumped plasticity model, and it also accounts for the interaction of axial force and bending moment. Strength and stiffness degradation are included through use of a damage-dependent constitutive relationship. A damage index is used to determine the onset of member failure. Following the failure of an element, the analysis continues in an efficient manner through use of a modified member stiffness procedure. This approach does not require the introduction of any additional degrees-of-freedom or modification of the element connectivity definitions. Finally, a methodology for updating the state of a structure at the time of member failure is presented. Analysis results indicate that dynamic redistribution of loads is a significant feature of the progressive collapse problem and should be accounted for in order to avoid estimates of capacity that are not conservative.


*Keywords:* Progressive collapse; Structural dynamics; Nonlinear analysis; Building collapse; Damage; Software

## 1. Introduction

Progressive collapse, characterized by widespread propagation of failure, can be triggered by the loss of a critical structural element or other localized damage to a structure. Of key importance is the concept that the resulting damage is disproportionate to the original cause. Progressive collapse of buildings has become an important issue for structural design since the collapse of the Ronan Point Apartment building in 1968. In this event, a gas explosion in an apartment near the top of the structure led to a vertical propagation of failures from the upper floors to the foundation. Although there has been a significant amount of research related to progressive collapse dating back to the early 1970s (e.g., Breen [1], Leyendecker and Ellingwood [2]), few researchers have considered the implications of dynamic load redistribution in the response of frame structures during a collapse event (Hakuno and Meguro [3], Isobe and Toi [4]). Furthermore, recent terrorist attacks against the Alfred P. Murrah Building in Oklahoma City in 1995, the US Embassy buildings in Africa in 1998, and the World Trade Center in New York in 1993 and 2001 have rekindled interest in the design of buildings to resist progressive collapse.

Based on research conducted during the 1970s, a direct design procedure known as the 'Alternate Load Path Method' was recommended as a simplified analysis technique for investigating the potential of progressive collapse in the design of building structures. Since then, this method has been integrated into several building codes and provisions (IBC [5], DoD [6], GSA [7]) for designing structures to resist progressive collapse. With the Alternate Load Path Method, one or more load carrying members are assumed to fail and are removed

* Corresponding author.

0045-7949/$ - see front matter © 2004 Elsevier Ltd. All rights reserved.
doi:10.1016/j.compstruc.2003.12.001

from the structural model for the purposes of analysis. The remaining structure is then analyzed to determine if other member failures result. Because progressive collapse is an extreme event with a low likelihood of occurrence, the design limit state is taken to be the prevention of widespread failure propagation. Accordingly, unfactored loads are used, and strength reduction factors are ignored. The procedure continues until there are no further member failures or the structure remains capable of supporting its loads despite the loss of various structural components. As a result of using the Alternate Load Path Method for progressive collapse analysis, information on static load redistribution for the structure under consideration is obtained. One criticism of this method is that it fails to consider dynamic effects that inevitably result following the failure of one or more load carrying members.

Pretlove et al. [8] discussed the importance of dynamic load redistribution in their research on the progressive failure of a tension spoke wheel. These researchers demonstrated that a static analysis predicting a damaged structure to be safe from progressive failure may not be conservative if inertial effects are taken into consideration. The authors (Kaewkulchai and Williamson [9]) also demonstrated the importance of considering inertial effects for frame structures through a simple frame example. Although dynamic effects on the response of truss structures during progressive failure have been presented in the research literature (Malla and Nalluri [10,11]), few researchers have considered dynamic load redistribution in the progressive collapse analysis of frame structures. In this paper, we present the development of a beam-column element for use in progressive collapse analysis of 2-D frames. For this research, inertial effects play a key role, and, thus, a solution methodology for tracking the dynamic response of a structure modeled with the developed beam-column element is presented. The procedure is computationally efficient and has the capability of determining the response of a frame in which members can fail at any time throughout the response history.

## 2. Beam element formulation

### 2.1. Inelastic beam-column element

The beam-column element originally developed by Kim [12] for the analysis of steel moment frames subjected to earthquake excitation forms the foundation of the element that was developed for the current study. The element employs a lumped plasticity model in which inelasticity is assumed to occur only at the element ends or hinges. In addition, the element utilizes a flexibility-based formulation which relies on force interpolation functions that satisfy the equilibrium of bending moments and axial force along the length of the element. In comparison, a stiffness-based element formulation would depend upon displacement interpolation functions that provide the necessary compatibility requirements. The effect of axial force on yield moment is also incorporated in the element formulation through a moment–axial force interaction relationship. To capture cyclic behavior, multi-linear force–deformation relationships, as well as the modified Mroz's hardening rule, are employed. For the current research, the original beam-column element was modified to account for large displacements through introduction of a geometric stiffness matrix. Thus, both nonlinear geometry (i.e., $P$–$\Delta$ effect) and nonlinear material behavior are considered.

### 2.2. Damage model

Many materials, including steel and concrete, experience strain softening under cyclic loading as a result of damage. The original beam-column element of Kim [12] incorporated these effects, in an empirical fashion, in the formulation of the constitutive model. Thus, damage and inelasticity effects were coupled in the original development. Various researchers, however, have proposed that these effects be treated independently, and observations of the response of various structural systems lend credibility to this approach. For example, it is possible for a brittle system to sustain severe damage yet show little plasticity. For this reason, the beam-column element of Kim was modified for the current research so that inelasticity and damage are considered separately. Therefore, to track the evolution of damage, a model representing its evolution is required.

Several damage models have been proposed in the literature that depend upon a damage index, $D$, having a value ranging from 0 (no damage) to 1 (total damage). Examples include those of Park and Ang [13] and Rao et al. [14] for concrete members, and models by Krawinkler and Zohrei [15], Ballio and Castiglioni [16], and Azevedo and Calado [17] for steel members. For the current research, we propose a formulation that depends linearly upon the maximum deformation and the accumulated plastic energy. To wit, damage, $D$, is given by the formula

$$D = \alpha U(\delta) + \beta W(\delta) \tag{1}$$

where $\alpha$, $\beta$ are constant (material) parameters, $U(\delta)$ is a function that depends upon the maximum deformation, and $W(\delta)$ is a function that depends upon the accumulated plastic energy.

By varying the values of $\alpha$ and $\beta$, one can represent different rates of damage accumulation so that many of the models presented in the literature can be represented (Williamson and Hjelmstad [18]). Because the damage-dependent response of frame members during a collapse

event is not known, the current model provides the flexibility to investigate the relative importance of the terms in the damage model. Thus, until data are available to suggest a model of damage that may be better suited to collapse analysis than the current model, the choice was made to use a simple model that could be varied so as to investigate how the evolution of damage affects the computed results. Therefore, unlike previous researchers, we allow $\alpha$ and $\beta$ to vary as a function of the properties of the structural system.

The use of a damage index to indicate failure is preferable to an arbitrary rule that may be based on some percentage reduction of strength or stiffness. Extending the basic model to account for both axial and rotational components, a modified damage index at each hinge can be expressed as

$$D_i = \alpha_i\left(\frac{\theta_{m_i}}{\theta_{y_i}} + \frac{\delta_{m_a}}{\delta_{y_a}} + \frac{\theta_{m_i}}{\theta_{y_i}}\frac{\delta_{m_a}}{\delta_{y_a}}\right) + \beta_i\left(\frac{\sum E_{p_i}}{E_{o_i}} + \frac{\sum E_{p_a}}{E_{o_a}} + \frac{\sum E_{p_i}}{E_{o_i}}\frac{\sum E_{p_a}}{E_{o_a}}\right) \quad (2)$$

where $\theta_m$, $\theta_y$ are the maximum and the yield rotations respectively, $\delta_{m_a}$, $\delta_{y_a}$ are the maximum and the yield axial displacements, respectively, and $E_o$ is the initial elastic energy prior to yield. The first two terms within each set of the parentheses in Eq. (2) represent a basic extension of the traditional Park and Ang [13] model in which damage is assumed to vary linearly as a function of maximum deformation and hysteretic energy dissipated. The last term within each set of parentheses accounts for coupling between axial and flexural behavior that is consistent with the constitutive model describing the behavior of the plastic hinges. While other forms of the damage index can be developed, the model adopted for the present study offers a simple, yet effective way to account for the degradation of structural properties. Moreover, the parameters $\alpha$ and $\beta$ can be calibrated with experimental data of impulsively loaded beams to represent variable rates of damage accumulation.

To incorporate the effects of stiffness and strength degradation at member hinges using the damage index, a simplified method suggested by Cipollina et al. [19] and Inglessis et al. [20] is implemented. With their approach, the stiffness matrix $\boldsymbol{K}$ of a beam member is obtained by inverting the member flexibility matrix $\boldsymbol{F}$, which includes a damage flexibility matrix $\boldsymbol{F}_d$. Thus,

$$\boldsymbol{K} = \boldsymbol{F}^{-1} \quad (3)$$

$$\boldsymbol{F} = \boldsymbol{F}_e + \boldsymbol{F}_p + \boldsymbol{F}_d \quad (4)$$

In Eq. (4), $\boldsymbol{F}_e$ is the elastic flexibility matrix, and $\boldsymbol{F}_p$ is the plastic flexibility matrix. The damage flexibility matrix $\boldsymbol{F}_d$, which is a function of damage indices and the elastic flexibility of a beam member, is given by

$$\boldsymbol{F}_d = \begin{bmatrix} \frac{D_a F_{e_{11}}}{(1-D_a)} & 0 & 0 \\ 0 & \frac{D_i F_{e_{22}}}{(1-D_i)} & 0 \\ 0 & 0 & \frac{D_j F_{e_{33}}}{(1-D_j)} \end{bmatrix} \quad (5)$$

where $D_i$ is the damage index at hinge $i$, $D_j$ is the damage index at hinge $j$, and $D_a$ is an axial damage index. The axial damage index $D_a$ is chosen as the larger value of $D_i$ and $D_j$ because we assume that, at the onset of failure, both the axial and rotational stiffness at the failed end go to zero, thereby implying separation of the failed member end from the remainder of the intact structure.

When $D_i$ or $D_j$ is nonzero, the member stiffness is modified. As discussed below, the damage indices are updated at each time step throughout the analysis procedure so that the development of damage affects the subsequent response as a function of time. Traditionally, damage indices are viewed as simply a quantification of a design limit state. If the damage index exceeds a certain value, then one concludes that a member or structure is no longer able to function within the design specifications. Under these circumstances, damage plays a passive role—damage is recorded, but it does not affect the evolution of the dynamic response. In this context there is no need for more than an indirect connection between physical damage and the damage index. In the present study, however, damage modifies the structural properties and hence contributes to the evolution of the response. While this concept is not new (see, for example, work by Baber and Wen [21]), it is one that has not been used directly to evaluate structural performance. Because we incorporate the damage index in the constitutive definition of the model, the stiffness of the beam member degrades as damage evolves. Note that for $D_i$ or $D_j = 1$, hinge $i$ or $j$ will have infinite flexibility (i.e., zero stiffness), and that hinge can be considered as "disconnected" or no longer attached to the structure. Thus, failure is assumed to take place at the member end in which the damage index has achieved a value of one.

In addition to stiffness degradation, the effect of strength degradation of the member is captured using the modified yield function as shown in Eq. (6).

$$\boldsymbol{f} = \left|\frac{\boldsymbol{M}}{(1-\boldsymbol{D})}\right| - \boldsymbol{M}_y \quad (6)$$

To illustrate the capabilities of the model, consider the response of the cantilever beam shown in Fig. 1(a). In this example, a W21×57 beam with $Mp = 4838$ k-in and $L = 96$ in, is subjected to a point load of $P = 40$ kips which is suddenly applied and then held constant throughout the duration of the response. Such a scenario may be representative of a failed element impacting a beam in a structure during a collapse event.

The response of the beam as a function of time, assuming values of the nodal mass to be 0.05 kips-s$^2$/in, is shown in Fig. 1(b) for different rates of damage

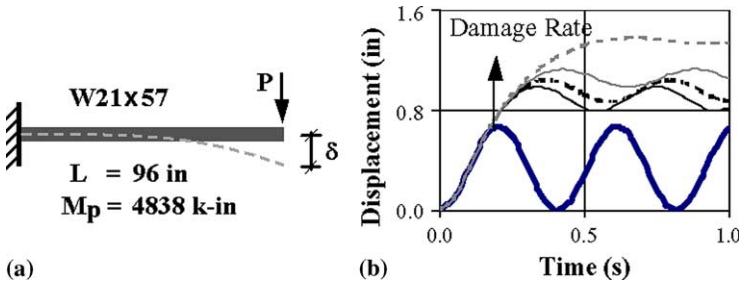


Fig. 1. (a) W21×57 cantilever beam with a suddenly applied point load $P$. (b) Tip displacement response history with increasing values of damage ($\alpha$, $\beta$).

accumulation. This figure shows a wide range of response parameters, ranging from zero damage (i.e., $\alpha = \beta = 0$), to severe damage ($\alpha = \beta = 0.09$ for this example). As might be expected, the response of the beam for this load case depends strongly upon the value of $\alpha$ but weakly upon $\beta$. For cyclic loading, however, $\beta$ plays an important role (Williamson [22]). Because the load scenario prior to the initiation of a progressive collapse event can vary widely, the choice was made to allow the damage model to depend upon the accumulated plastic energy. While progressive collapse can be initiated by blast or impact, some researchers have proposed that, in the context of retrofitting older structures in areas of high seismicity, it may also occur as the result of an earthquake (Moehle et al. [23]). In many cases, the costs associated with strengthening all the columns in a building located in an earthquake-prone region are prohibitive, and designers count on system redundancy so that selected columns can be strengthened while others are left in their original state. As such, it is possible for collapse to initiate due to the failure of an unprotected column, and it is important to have a damage model that accounts for cyclic loads so that the state of the structure prior to the onset of collapse can be captured accurately.

As seen in Fig. 1(b), faster rates of damage accumulation (i.e., $\alpha$ and $\beta$ increasing) give larger displacements and also provide more damping to the system. Using the calculated tip displacements and end moments, moment–rotation ($M$–$\theta$) relationships of the support end for different rates of damage can be plotted as shown in Fig. 2. For comparison, the response of the beam has also been computed for the applied cyclic displacement history shown in Fig. 3. Plots of applied force versus deflection are shown in Fig. 4. The results shown in Figs. 1(b), 2, and 4 demonstrate the sensitivity of the response to the values of $\alpha$ and $\beta$. These graphs also give a clear view of the strength and stiffness degradation of the beam hinge for different rates of damage accumulation. Clearly, the response demonstrated by the element is strongly dependent upon its loading history.

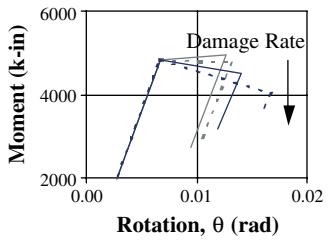


Fig. 2. Moment–rotation ($M$–$\theta$) relationships for different rates of damage ($\alpha$, $\beta$).

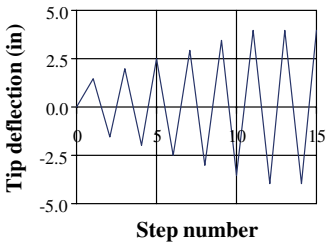


Fig. 3. Deflection input history for the W21×57 cantilever beam.

### 2.3. Member loads

In the analysis of frame structures by the stiffness method, loads acting on a member need to be replaced by equivalent joint loads through the use of fixed end forces, $\boldsymbol{R}_{\mathrm{F}}$. It is important to discuss the role of the fixed end forces in computing the final internal forces of a member, $\boldsymbol{R}$, using the equation

$$\boldsymbol{R} = \boldsymbol{K} \cdot \boldsymbol{u} + \boldsymbol{R}_{\mathrm{F}} \tag{7}$$

where $\boldsymbol{K}$ is the member stiffness matrix and $\boldsymbol{u}$ is the displacement vector of the member. The fixed end forces $\boldsymbol{R}_{\mathrm{F}}$ of an elastic member for various types of member loads can be easily found in the literature (i.e., Felton and Nelson [24]). The relationship in Eq. (7) is appli-

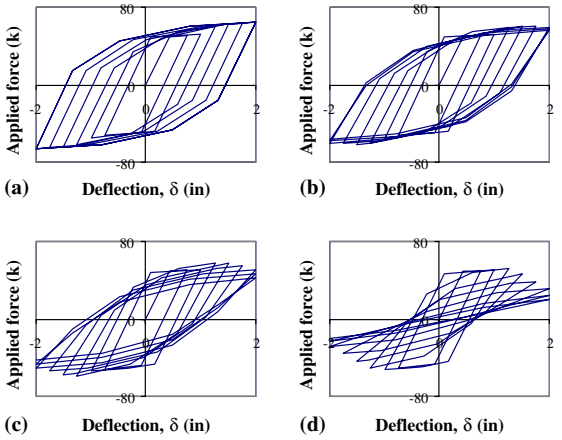


Fig. 4. Response of the damaged cantilever beam with different rates of damage ($\alpha$, $\beta$). (a) No damage ($\alpha = \beta = 0$), (b) slow damage ($\alpha = \beta = 0.01$), (c) moderate damage ($\alpha = \beta = 0.03$), (d) severe damage ($\alpha = \beta = 0.1$).

cable for calculating elastic member forces, and it is commonly employed in matrix analysis of frame structures.

For inelastic response, however, using the conventional fixed end forces, $\boldsymbol{R}_{\mathrm{F}}$, can lead to a violation of the yield function at the member ends because the sum of the elastic $\boldsymbol{R}_{\mathrm{F}}$ and $\boldsymbol{K} \cdot \boldsymbol{u}$ may lead to internal forces $\boldsymbol{R}$ that exceed the yield limit. This problem becomes an issue during the element state determination as described in Section 3.2. In general, the fixed end forces are dependent upon the hinge stiffness, and the magnitude of the fixed end forces should vary as the stiffness of the hinges at the member ends change. Fig. 5 shows the fixed end forces, $\boldsymbol{R}^*_{\mathrm{F}}$, for a beam element in which the inelasticity of the member is accounted for by springs with stiffness $k_1$ and $k_2$ at each hinge.

For elastic response, $k_1 = k_2 = \infty$, and $\boldsymbol{R}^*_{\mathrm{F}} = \boldsymbol{R}_{\mathrm{F}}$ (reactions of a fixed–fixed beam). When $k_1 = k_2 = 0$, plastic hinges have formed at both member ends, and $\boldsymbol{R}^*_{\mathrm{F}}$ corresponds to the reactions of a simply supported beam. To derive the fixed end forces $\boldsymbol{R}^*_{\mathrm{F}}$ for intermediate values of stiffness, one can start by solving the Euler–Bernoulli beam equation for a flexural member with end springs and a uniform load $q_0$. The four boundary

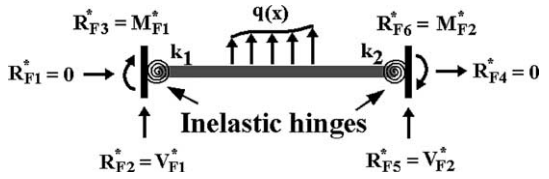


Fig. 5. An inelastic beam member with fixed end forces $\boldsymbol{R}^*_{\mathrm{F}}$.

conditions associated with the above example, assuming constant EI, are

$$w(0) = 0 \quad \text{and} \quad \mathrm{EI}w''(0) = k_1\theta_1 \quad \text{at } x = 0 \tag{8a}$$

$$w(L) = 0 \quad \text{and} \quad \mathrm{EI}w''(L) = -k_2\theta_2 \quad \text{at } x = L \tag{8b}$$

where $\theta_1 = w'(0)$, and $\theta_2 = w'(L)$ for the Euler–Bernoulli assumptions (i.e., no shear deformations). Introducing the parameters $\lambda_1$ and $\lambda_2$ through Eq. (9)

$$k_1 = \lambda_1 \frac{\mathrm{EI}}{L} \quad \text{and} \quad k_2 = \lambda_2 \frac{\mathrm{EI}}{L} \tag{9}$$

the governing differential equation can be solved by successive integration to obtain the following equations:

$$\mathrm{EI}w(x) = q_0 \frac{x^4}{24} + C_1 \frac{x^3}{6} + C_2 \frac{x^2}{2} + C_3 x \tag{10a}$$

$$C_1 = -\frac{q_0 L}{4} - \frac{q_0 L}{4} \frac{(12 + 6\lambda_1 + 2\lambda_2 + \lambda_1\lambda_2)}{(12 + 4\lambda_1 + 4\lambda_2 + \lambda_1\lambda_2)} \tag{10b}$$

$$C_2 = \frac{q_0 L^2}{12} \frac{(6\lambda_1 + \lambda_1\lambda_2)}{(12 + 4\lambda_1 + 4\lambda_2 + \lambda_1\lambda_2)} \tag{10c}$$

$$C_3 = \frac{q_0 L^3}{12} \frac{(6 + \lambda_2)}{(12 + 4\lambda_1 + 4\lambda_2 + \lambda_1\lambda_2)} \tag{10d}$$

Finally, the fixed end forces can be found by differentiating Eq. (10a).

Generally, only the fixed end moments $M^*_{\mathrm{F1}}$ and $M^*_{\mathrm{F2}}$ are needed because the fixed end shears $V^*_{\mathrm{F1}}$ and $V^*_{\mathrm{F2}}$ can always be obtained by consideration of equilibrium for the beam member. Solving for the end moments yields the following results:

$$M^*_{\mathrm{F1}} = \frac{q_0 L^2}{12} \frac{(6\lambda_1 + \lambda_1\lambda_2)}{(12 + 4\lambda_1 + 4\lambda_2 + \lambda_1\lambda_2)} \tag{11a}$$

$$M^*_{\mathrm{F2}} = -\frac{q_0 L^2}{12} \frac{(6\lambda_2 + \lambda_1\lambda_2)}{(12 + 4\lambda_1 + 4\lambda_2 + \lambda_1\lambda_2)} \tag{11b}$$

Note that, for an elastic member, $M_{\mathrm{F1}} = q_0 L^2/12$ and $M_{\mathrm{F2}} = -q_0 L^2/12$. Therefore, Eqs. (11a) and (11b) become

$$M^*_{\mathrm{F1}} = \frac{(6\lambda_1 M_{\mathrm{F1}} - \lambda_1\lambda_2 M_{\mathrm{F2}})}{(12 + 4\lambda_1 + 4\lambda_2 + \lambda_1\lambda_2)} \tag{12a}$$

$$M^*_{\mathrm{F2}} = \frac{(6\lambda_2 M_{\mathrm{F2}} - \lambda_1\lambda_2 M_{\mathrm{F1}})}{(12 + 4\lambda_1 + 4\lambda_2 + \lambda_1\lambda_2)} \tag{12b}$$

The same derivation for an inelastic beam member with other types of member loads (i.e., concentrated and trapezoidal loads can also be accomplished). Regardless of the loading scenario, the final equations will be exactly as those appearing in Eqs. (12a) and (12b), where, in general, $M_{\mathrm{F1}}$ and $M_{\mathrm{F2}}$ represent the elastic fixed end

moments for the load case under consideration. Once the fixed end moments have been computed, the fixed end shears can be obtained by considering equilibrium of the inelastic beam member. By using the modified fixed-end forces $\boldsymbol{R}_{\mathrm{F}}^{*}$ when computing inelastic member forces, the problem of violating the yield function at the ends of a member is avoided.

## 3. Solution procedure

In this section, a detailed description of the methodology used to develop the computer program for progressive collapse analysis of planar frame structures is given.

### 3.1. Solution method

The solution methodology incorporates an implicit direct integration scheme, the Newmark-beta method (Newmark [25]), for solving the governing equations of equilibrium described by Eq. (13).

$$\boldsymbol{M}\boldsymbol{U}'' + \boldsymbol{C}\boldsymbol{U}' + \boldsymbol{R}^{\mathrm{Int}} = \boldsymbol{R}^{\mathrm{Ext}} \tag{13}$$

In Eq. (13), $\boldsymbol{U}$, $\boldsymbol{U}'$ and $\boldsymbol{U}''$ are the displacement, velocity and acceleration vectors, respectively, $\boldsymbol{M}$ and $\boldsymbol{C}$ are the system mass and damping matrices, respectively, and $\boldsymbol{R}^{\mathrm{Int}}$ and $\boldsymbol{R}^{\mathrm{Ext}}$ are the internal and external force vectors. For every time step, the well-known Newton–Raphson method is employed for solving the nonlinear system of equations. Details of the methodology can be found in many references including Bathe [26], Belytschko et al. [27], etc.

### 3.2. Element state determination

As described earlier, the beam-column element used in the current study is a flexibility-based element in which, during the determination of its internal forces, equilibrium rather than compatibility is satisfied. The determination of the element forces employs the current element deformations in conjunction with the element stiffness matrix obtained from the last converged iteration step. More information on flexibility-based elements can be found in the literature (e.g., Spacone et al. [28], Neuenhofer and Filippou [29]).

Generally, a planar beam element consists of 6 degrees of freedom (often referred to as the "complete set") including two translations and one rotational displacement at each end ($u_1$–$u_6$), as shown in Fig. 6. In a flexibility-based formulation, however, rigid body motions need to be removed. Hence, the element response can be described in terms of only three independent degrees of freedom (referred to as the "essential set"). Thus, only the axial deformation and two rotational

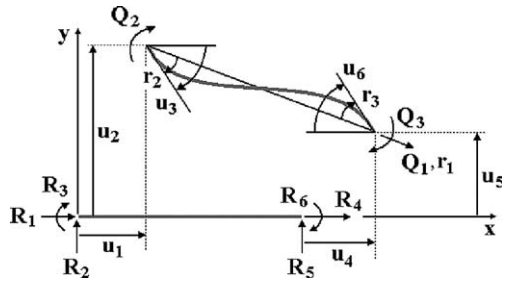


Fig. 6. Element degrees of freedom for complete and essential sets.

deformations ($r_1$–$r_3$) are needed. Other force–deformation variables can be used; the critical requirement is that the system under consideration be free of rigid body motion. For the beam element shown in Fig. 6, the relative element forces associated with the essential set are denoted by $Q_1$, $Q_2$, and $Q_3$.

From linear geometry theory, the relationship between member displacements and member deformations can be determined from the following expression

$$\boldsymbol{r} = \boldsymbol{A} \cdot \boldsymbol{u} \tag{14}$$

where $\boldsymbol{A}$ = the kinematic transformation matrix

$$= \begin{bmatrix} -1 & 0 & 0 & 1 & 0 & 0 \\ 0 & -1/L & 1 & 0 & 1/L & 0 \\ 0 & -1/L & 0 & 0 & 1/L & 1 \end{bmatrix}$$

Subsequently, the internal forces associated with the complete set $\boldsymbol{R}$ can be obtained from the relative element forces by

$$\boldsymbol{R} = \boldsymbol{A}^{\mathrm{T}} \cdot \boldsymbol{Q} \tag{15}$$

The following determination of the relative element forces $\boldsymbol{Q}$ is with respect to an iteration step $i$ in the Newton–Raphson method during an incremental time step of the Newmark-beta method.

1. Calculate the element deformation increments $\Delta \boldsymbol{r}^i = \boldsymbol{A} \cdot \Delta \boldsymbol{u}^i$.
2. Calculate the relative element force increments $\Delta \boldsymbol{Q}^i = \boldsymbol{K}_{\mathrm{t}}^{i-1} \cdot \Delta \boldsymbol{r}^i$.
3. Check if the current element forces $\boldsymbol{Q}^i = \boldsymbol{Q}^{i-1} + \Delta \boldsymbol{Q}^i$ violate yield functions
   (i) If there is no yielding, continue to Step 9.
   (ii) If yielding occurs, calculate a factor 'FAC' (Fig. 7) for each yielded hinge as follows:

$$\mathrm{FAC} = \frac{\sqrt{(M_{\mathrm{y}} - M)^2 + (F_{\mathrm{y}} - F)^2}}{\sqrt{(\mathrm{d}M)^2 + (\mathrm{d}F)^2}}$$

   where $\mathrm{d}M$ and $\mathrm{d}F$ are the moment and axial force increments at the yielded hinge.

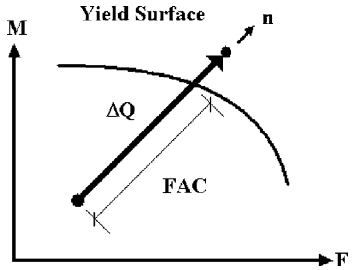


Fig. 7. Yield surface and element force increments.

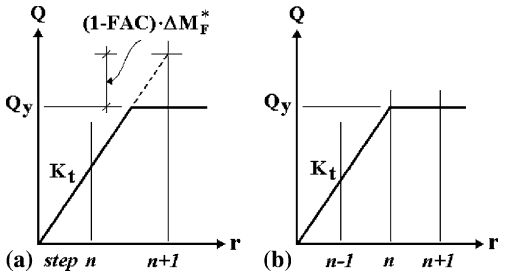


Fig. 8. An element force increment with elastic–perfectly plastic material behavior. (a) Yielding during an incremental step, (b) yielding at the end of an incremental step.

(iii) Calculate the hinge flexibility matrix, $\boldsymbol{F}_{\mathrm{h}}$, at each hinge to account for yielding

$$\boldsymbol{F}_{\mathrm{h}} = \frac{\boldsymbol{n}\boldsymbol{n}^{\mathrm{T}}}{\boldsymbol{n}^{\mathrm{T}}\boldsymbol{K}_{\mathrm{p}}\boldsymbol{n}}$$

where $\boldsymbol{K}_{\mathrm{p}}$ is the diagonal plastic stiffness matrix of the hinge. The plastic flexibility matrix, $\boldsymbol{F}_{\mathrm{p}}$, is obtained as

$$\boldsymbol{F}_{\mathrm{p}} = \boldsymbol{F}_{\mathrm{h}_i} + \boldsymbol{F}_{\mathrm{h}_j}$$

(iv) Update the element flexibility matrix, $\boldsymbol{F}$

$$\boldsymbol{F} = \boldsymbol{F}_{\mathrm{e}} + \boldsymbol{F}_{\mathrm{p}} + \boldsymbol{F}_{\mathrm{d}}$$

4. Obtain the partial force increments $\Delta\boldsymbol{Q}^i = \mathrm{FAC} \cdot \Delta\boldsymbol{Q}^i$.
5. Calculate the remaining deformation increments $\Delta\hat{\boldsymbol{r}}^i = (1 - \mathrm{FAC}) \cdot \Delta\boldsymbol{r}^i$.
6. Update the current stiffness matrix $\widehat{\boldsymbol{K}}_{\mathrm{t}}^{i-1} = \boldsymbol{F}^{-1}$.
7. Obtain the additional force increments $\Delta\widehat{\boldsymbol{Q}}^i = \widehat{\boldsymbol{K}}_{\mathrm{t}}^{i-1} \cdot \Delta\hat{\boldsymbol{r}}^i$.
8. Repeat Step 3.
9. Calculate the internal element forces $\boldsymbol{R}^i = \boldsymbol{A}^{\mathrm{T}} \cdot \boldsymbol{Q}^i$.

In this procedure, it is important to note that fixed end forces for an element with member loads have not yet been included. To account for fixed end forces, the equations presented in Steps 2 and 7 need to be modified. The required equations are expressed as

$$\Delta\boldsymbol{Q}^i = \boldsymbol{K}_{\mathrm{t}}^{i-1} \cdot \Delta\boldsymbol{r}^i + \Delta\boldsymbol{M}_{\mathrm{F}}^{*} \tag{16}$$

$$\Delta\widehat{\boldsymbol{Q}}^i = \widehat{\boldsymbol{K}}_{\mathrm{t}}^{i-1} \cdot \Delta\hat{\boldsymbol{r}}^i + (1 - \mathrm{FAC}) \cdot \Delta\boldsymbol{M}_{\mathrm{F}}^{*} \tag{17}$$

where $\Delta\boldsymbol{M}_{\mathrm{F}}^{*} = \{\,0 \quad \Delta M_{\mathrm{F1}}^{*} \quad \Delta M_{\mathrm{F2}}^{*}\,\}^{\mathrm{T}}$ is a vector of fixed end forces that are calculated, as described previously, to account for the hinge properties at the member ends.

To illustrate the significance of using the modified fixed end forces $\boldsymbol{M}_{\mathrm{F}}^{*}$ as described above, consider the response of an elastic–perfectly plastic material as shown in Fig. 8(a). For such a case, the remaining portion of fixed end forces, $(1 - \mathrm{FAC}) \cdot \Delta\boldsymbol{M}_{\mathrm{F}}^{*}$ cannot be applied to $\Delta\widehat{\boldsymbol{Q}}^i$ because yielding of the material requires no additional forces. Note that if the end of an incremental step gives exactly the yielding point as shown in Fig. 8(b), Eq. (17) is no longer needed. Nevertheless, a problem still occurs in the next time step when using elastic fixed end forces because of the same reason that yielding requires no additional forces. To overcome this difficulty, the modified fixed end forces as described in Section 2.3 are used so that the problem is automatically resolved. If at the end of an incremental step the yield point has not been computed exactly (Fig. 8(a)), one can iterate on the time step size until this situation is achieved. This approach, however, is computationally intensive as it requires an iterative solution strategy, and yielding can happen often during the course of an analysis. To solve this problem effectively, a solution based on equivalent deformations is proposed.

Considering Eq. (16), the equivalent deformation increments $\Delta\boldsymbol{r}_{\mathrm{e}}^i$, in conjunction with the current element stiffness matrix $\boldsymbol{K}_{\mathrm{t}}^{i-1}$, will need to give the same relative force increments $\Delta\boldsymbol{Q}^i$. Therefore, $\Delta\boldsymbol{r}_{\mathrm{e}}^i$ can be obtained by the expression

$$\Delta\boldsymbol{r}_{\mathrm{e}}^i = [\boldsymbol{K}_{\mathrm{t}}^{i-1}]^{-1}\{\boldsymbol{K}_{\mathrm{t}}^{i-1} \cdot \Delta\boldsymbol{r}^i + \Delta\boldsymbol{M}_{\mathrm{F}}^{*}\} \tag{18}$$

With only minor modification, the element state determination can then be accomplished using Steps 1–9 as described earlier by using Eq. (16) and adding the calculation of $\Delta\boldsymbol{r}_{\mathrm{e}}^i$ in Step 2.

The following example demonstrates the procedure for the state determination of an element with a uniform load $q_0$. The example is a fixed–fixed beam consisting of two equal length elements. Because of symmetry, there is only one degree of freedom, the vertical displacement $U_1$, as seen in Fig. 9(a). The solution, including bending moment and shear diagrams, is shown in Fig. 9(b). Note that yielding takes place at the middle node.

The procedure starts by using conventional matrix structural analysis to obtain the displacement $U_1 = \Delta U_1 = 21093.75/\mathrm{EI}$ for the fixed–fixed beam with $\Delta q_0 = 10$ kips. In this case, only one incremental step is required. For the element state determination, consider element #1,

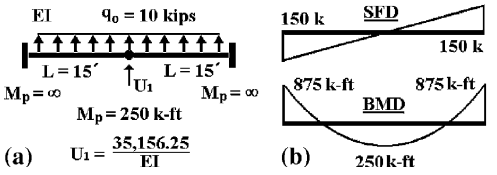


Fig. 9. (a) A fixed–fixed beam with a uniform load, (b) bending moment and shear diagrams.

1. Calculate $\Delta \boldsymbol{r}^1 = \boldsymbol{A} \cdot \Delta \boldsymbol{u}^1 = \frac{1406.25}{EI} \begin{Bmatrix} 1 \\ 1 \end{Bmatrix}$ ft.
2. Calculate $\Delta \boldsymbol{Q}^1 = \boldsymbol{K}_t \cdot \Delta \boldsymbol{r}^1 + \Delta \boldsymbol{M}_F^* = \begin{Bmatrix} 562.5 \\ 562.5 \end{Bmatrix} + \begin{Bmatrix} 187.5 \\ -187.5 \end{Bmatrix} = \begin{Bmatrix} 750 \\ 375 \end{Bmatrix}$ k-ft.
   Obtain $\Delta \boldsymbol{r}_e^1 = \boldsymbol{K}_t^{-1} \cdot \Delta \boldsymbol{Q}^1 = \frac{2812.5}{EI} \begin{Bmatrix} 1 \\ 0 \end{Bmatrix}$ ft.
3. Check for yielding: $\boldsymbol{Q} = \Delta \boldsymbol{Q}^1$; 375 k-ft > 250 k-ft, yielded.
   Calculate FAC $= \frac{250}{375} = 0.6667$.
4. Therefore, $\Delta \boldsymbol{Q}^1 = \text{FAC} \cdot \Delta \boldsymbol{Q}^1 = \begin{Bmatrix} 500 \\ 250 \end{Bmatrix}$ ft.
5. Calculate $\Delta \hat{\boldsymbol{r}}^1 = (1 - \text{FAC}) \cdot \Delta \boldsymbol{r}_e^1 = \frac{937.5}{EI} \begin{Bmatrix} 1 \\ 0 \end{Bmatrix}$ ft.
6. Update $\widehat{\boldsymbol{K}}_t = \frac{3EI}{L} \begin{bmatrix} 1 & 0 \\ 0 & 0 \end{bmatrix}$.
7. Calculate $\Delta \widehat{\boldsymbol{Q}}^1 = \widehat{\boldsymbol{K}}_t \cdot \Delta \hat{\boldsymbol{r}}^1 = \begin{Bmatrix} 187.5 \\ 0 \end{Bmatrix}$ k-ft.
8. Check for yielding: $\boldsymbol{Q} = \boldsymbol{Q} + \Delta \widehat{\boldsymbol{Q}}^1 = \begin{Bmatrix} 687.5 \\ 250 \end{Bmatrix}$ k-ft; no yielding.
9. Calculate $\boldsymbol{R} = \boldsymbol{A}^T \cdot \boldsymbol{Q} + \boldsymbol{V}_F^* = \begin{Bmatrix} -62.5 \\ 687.5 \\ 62.5 \\ 250 \end{Bmatrix} + \begin{Bmatrix} -75 \\ 0 \\ -75 \\ 0 \end{Bmatrix} = \begin{Bmatrix} -137.5 \\ 687.5 \\ -12.5 \\ 250 \end{Bmatrix}$.

For element #2, the same procedure is applied and the same results are achieved due to symmetry. The next step is to check for equilibrium of the system. For this example, one need only consider nodal equilibrium of the center node. At this location, the system is out of equilibrium by 25 kips. Therefore, a 2nd iteration is needed for the beam with a point load of 25 kips acting at the center node. From the matrix analysis, the additional displacement is calculated as $\Delta U_1 = 14062.5/EI$ ft, and the additional member forces are computed to be $\Delta \boldsymbol{R} = \{-12.5, 187.5, 12.5, 0\}^T$. Hence, $U_1 = U_1 + \Delta U_1 = 35156.25/EI$ ft, and

$$\boldsymbol{R} = \boldsymbol{R} + \Delta \boldsymbol{R} = \begin{Bmatrix} -150 \\ 875 \\ 0 \\ 250 \end{Bmatrix}$$

which give the same results as given in Fig. 9(b).

### 3.3. Member failure

During an analysis, the damage index $D$ is used to determine the onset of member failure. Because each hinge of a member experiences different load and deformation histories, failure of member ends can happen at different times. As described in Section 2.2, when the damage index of a hinge reaches a value of one, the hinge may be assumed to separate completely from the main structure (i.e., strength and stiffness are reduced to zero). At this point, the failed hinge becomes discontinuous from its primary joint, but the hinge on the opposite end of the member can still be intact. To continue the analysis after failure of member hinges, an additional node at the failed hinge may be introduced. Because three new degrees of freedom are added to the structure, the system of equations becomes larger. Hence, the analysis will require more computational effort, particularly when there are many failed hinges. In addition, changing the dimensions of all matrices is required, resulting in expensive computer time for transferring data between matrices. Also, new definitions for element connectivity must be established. As a result of the drawbacks associated with adding a new node to the definition of the structural model, in the current computer program the analysis continues in an efficient manner through the use of a modified member stiffness procedure with releases of end forces. A subroutine for substructure analysis of failed members is implemented to achieve this goal. Systematically, this approach provides a convenient means of keeping track of all failed members, and the main analysis routine is not greatly altered.

The modified member stiffness approach utilizes a condensation process of the stiffness matrix based on equilibrium of the member for degrees of freedom that are released. The static condensation process for a beam element is common and generally found in structural analysis textbooks (i.e., Felton and Nelson [24]). For the problem considered, all three degrees of freedom at either end of an element are released because of the failure of the end. When releasing one end, the element forces at the released end become zero. Moreover, the released end displacements can be determined from the remaining end displacements and the applied forces through use of the modified of the element stiffness matrix. Note that the fixed end force vector $\boldsymbol{R}_F$ must also be modified to reflect the change of end conditions.

For illustrative purpose, assume that failure takes place at the right end of a beam-column element. For this case, the incremental equilibrium equations of the element can be written as

$$\begin{Bmatrix} \Delta \boldsymbol{R}_c \\ \Delta \boldsymbol{R}_r \end{Bmatrix} = \begin{bmatrix} \boldsymbol{K}_{cc} | \boldsymbol{K}_{cr} \\ \boldsymbol{K}_{rc} | \boldsymbol{K}_{rr} \end{bmatrix} \begin{Bmatrix} \Delta \boldsymbol{u}_c \\ \Delta \boldsymbol{u}_r \end{Bmatrix} + \begin{Bmatrix} \Delta \boldsymbol{R}_{Fc} \\ \Delta \boldsymbol{R}_{Fr} \end{Bmatrix} \tag{19}$$

where subscripts $c$ and $r$ refer to 'contracted' and 'released' respectively. The contracted set consists of incremental force and displacement vectors corresponding to the element degrees of freedom 1 through 3 at the intact end. Likewise, the released set contains those for the element degrees of freedom 4 through 6 at the released end. Because the released element force vector $\Delta \boldsymbol{R}_r$ is zero, the released displacement vector $\Delta \boldsymbol{u}_r$ can be written in terms of $\Delta \boldsymbol{u}_c$ as

$$\Delta \boldsymbol{u}_r = -[\boldsymbol{K}_{rr}]^{-1}[\boldsymbol{K}_{rc}\Delta \boldsymbol{u}_c + \Delta \boldsymbol{R}_{Fr}] \tag{20}$$

As a result, the incremental equilibrium equations for the contracted set can be expressed by

$$\Delta \boldsymbol{R}_c = \overline{\boldsymbol{K}}_{cc}\Delta \boldsymbol{u}_c + \Delta \overline{\boldsymbol{R}}_{Fc} \tag{21}$$

where $\overline{\boldsymbol{K}}_{cc} = [\boldsymbol{K}_{cc} - \boldsymbol{K}_{cr}\boldsymbol{K}_{rr}^{-1}\boldsymbol{K}_{rc}]$ is the modified member stiffness matrix, and $\Delta \overline{\boldsymbol{R}}_{Fc} = [\Delta \boldsymbol{R}_{Fc} - \boldsymbol{K}_{cr}\boldsymbol{K}_{rr}^{-1}\Delta \boldsymbol{R}_{Fr}]$ is the modified fixed-end force vector.

It is interesting to observe that the relationships derived in Eqs. (20) and (21) are based on static equilibrium of the element, and therefore do not apply for dynamic analyses. However, if the Newmark-beta method is employed, similar equations, which are valid for dynamic analyses, can be developed because the relationship among displacement, velocity, and acceleration is assumed known. Thus, the governing equations of dynamic equilibrium can be cast in terms of unknown displacements. Accordingly, inertial effects in the response are accounted for, and the procedure outlined above can be used with only slight modification.

The incremental equations of motion for a dynamic system, when combined with the Newmark-beta method, can be written as

$$\Delta \boldsymbol{P}_{eff} = \boldsymbol{K}_{eff}\Delta \boldsymbol{U} \tag{22}$$

in which $\boldsymbol{K}_{eff}$ and $\Delta \boldsymbol{P}_{eff}$ are expressed by

$$\boldsymbol{K}_{eff} = A_1\boldsymbol{M} + A_4\boldsymbol{C} + \boldsymbol{K} \tag{23}$$

$$\Delta \boldsymbol{P}_{eff} = \Delta \boldsymbol{P} + \boldsymbol{M}[A_2\boldsymbol{v} + A_3\boldsymbol{a}] + \boldsymbol{C}[A_5\boldsymbol{v} + A_6\boldsymbol{a}] \tag{24}$$

where $A_1$–$A_6$ are the Newmark time integration constants, $\boldsymbol{v}$ is the velocity vector, and $\boldsymbol{a}$ is the acceleration vector. Because Eq. (22) is expressed in a form comparable to Eq. (19), the released displacement vector $\Delta \boldsymbol{u}_r$ from Eq. (20) can be rewritten as

$$\Delta \boldsymbol{u}_r = -[\boldsymbol{K}_{eff_{rr}}]^{-1}[\boldsymbol{K}_{eff_{rc}}\Delta \boldsymbol{u}_c + \Delta \boldsymbol{R}_{eff_{Fr}}] \tag{25}$$

The derived equation for $\Delta \boldsymbol{u}_r$ is now based on dynamic equilibrium, and therefore, inertial effects are accounted for by using $\boldsymbol{K}_{eff}$ and $\Delta \boldsymbol{R}_{eff_F}$. Because the fixed end forces are the negative values of the applied forces, the effective fixed end force vector, $\Delta \boldsymbol{R}_{eff_F}$, similarly to $\Delta \boldsymbol{P}_{eff}$ is given as

$$\Delta \boldsymbol{R}_{eff_F} = \Delta \boldsymbol{R}_F - \boldsymbol{M}[A_2\boldsymbol{v} + A_3\boldsymbol{a}] - \boldsymbol{C}[A_5\boldsymbol{v} + A_6\boldsymbol{a}] \tag{26}$$

Based on the discussion above, together with Eqs. (21), (23) and (26), the procedure for dynamic progressive collapse analysis with the modified member stiffness approach only involves modification of the stiffness matrix and fixed end forces of a failed member. Thus, Eq. (21) can be employed with the modified member stiffness matrix $\overline{\boldsymbol{K}}_{cc}$ and the modified fixed-end force vector $\Delta \overline{\boldsymbol{R}}_{Fc}$. These matrices correspond to the contracted degrees of freedom at the intact end, and they can be determined form Eqs. (27) and (28).

$$\overline{\boldsymbol{K}}_{cc} = [\boldsymbol{K}_{eff_{cc}} - \boldsymbol{K}_{eff_{cr}}\boldsymbol{K}_{eff_{rr}}^{-1}\boldsymbol{K}_{eff_{rc}}] \tag{27}$$

$$\Delta \overline{\boldsymbol{R}}_{Fc} = [\Delta \boldsymbol{R}_{eff_{Fc}} - \boldsymbol{K}_{eff_{cr}}\boldsymbol{K}_{eff_{rr}}^{-1}\Delta \boldsymbol{R}_{eff_{Fr}}] \tag{28}$$

With $\overline{\boldsymbol{K}}_{cc}$ and $\Delta \overline{\boldsymbol{R}}_{Fc}$, analysis after member failure can continue with little modification to the main analysis routine because no new degrees of freedom are added to the system. At the end of a converged time step, the released displacement vector $\Delta \boldsymbol{u}_r$ at the failed end of the member can be obtained from the contracted displacement vector $\Delta \boldsymbol{u}_c$ at the intact end using Eq. (25). Thus, using the approach just outlined, the assembly process for the stiffness matrix and the applied force vector of the main structure does not change. In addition, the equation solver still determines the same number of unknown degrees of freedom. Accordingly, the approach is computationally efficient.

To verify the modified member stiffness approach, results obtained from a dynamic analysis using this approach are compared with those obtained from a conventional dynamic analysis. For this purpose, the system shown in Fig. 10(a) is considered. The system is a fixed–fixed beam consisting of two elements and two degrees of freedom as shown. A point load $P$ of 20 kips acts at Node 2. For static equilibrium, the system has shear and moment diagrams as shown in Fig. 10(b). To illustrate the modified member stiffness method, the right end of member 2 is assumed to fail abruptly so that the support is no longer available to resist loads. For a conventional dynamic analysis, new degrees of freedom at Node 3 would need to be introduced. Hence, after failure at Node 3, the structure can be analyzed by using a system having four degrees of freedom with suddenly applied forces $S$ and $M$ at Node 3 as shown in Fig. 11. For this example, $S = 10$ kips and $M = 300$ k-in. For a dynamic

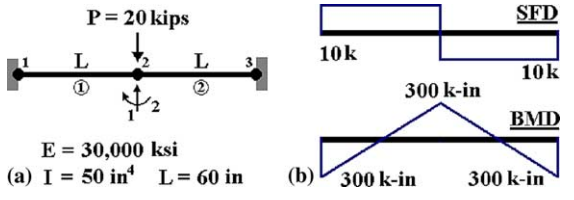


Fig. 10. (a) A system with failure at Node 3, (b) bending moment and shear diagrams.

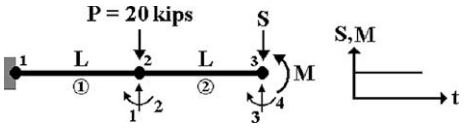


Fig. 11. An equivalent system with a suddenly applied force.

analysis using the modified member stiffness approach, only two degrees of freedom are required because no new degrees of freedom are introduced to the system. The response at the failed end can be obtained through Eq. (25).

For the dynamic analyses performed, $\Delta t = 0.01$ s and mass = 0.05 kips-s$^2$/in at each member end. In addition, rotational inertia and damping are ignored. The results obtained from a conventional dynamic analysis and a dynamic analysis using the modified member stiffness approach are compared in Fig. 12. As seen in the graphs, the differences between the displacement response histories obtained from the conventional dynamic analysis and the modified member stiffness approach are negligible. Similarly, bending moments of members 1 and 2 obtained from the two approaches are nearly identical. Hence, applying the modified member stiffness approach results in a simple, yet efficient routine for analyses of frame structures after member failure.

One important issue that needs to be addressed is the impact of failed members on other portions of the remaining structure. When a member fails, whether at one or both ends, the failed ends move independently from the main structure. Therefore, this member may come into contact with another member. When contact occurs, additional mass and impact forces are imposed on the main structure. Currently, a solution method to account for these effects is being studied and implemented into the computer program.

### 3.4. Updating

Generally, in nonlinear dynamic analyses using the incremental equations of motion, member stiffness matrices, as well as displacement, velocity and acceleration vectors are updated at the end of each converged time step. The stiffness matrix of a member is updated to account for material and geometric nonlinearities, while the displacement, velocity, and acceleration vectors are updated to satisfy the equilibrium equations. Once the solution (increments in the displacement vectors $\Delta \boldsymbol{U}_n$) is obtained at an incremental time step $n$ using the Newmark-beta method, the displacement, velocity, and acceleration vectors at time $t_{n+1}$ are updated as follows,

$$\boldsymbol{U}_{n+1} = \boldsymbol{U}_n + \Delta \boldsymbol{U}_n \tag{29}$$

$$\boldsymbol{v}_{n+1} = \boldsymbol{v}_n + A_4 \Delta \boldsymbol{U}_n - A_5 \boldsymbol{v}_n - A_6 \boldsymbol{a}_n \tag{30}$$

$$\boldsymbol{a}_{n+1} = \boldsymbol{a}_n + A_1 \Delta \boldsymbol{U}_n - A_2 \boldsymbol{v}_n - A_3 \boldsymbol{a}_n \tag{31}$$

Additional updating schemes, however, are required at the time of member failure. Considering a node at the point of intersection between one beam and two columns, fracture is assumed to occur at the beam hinge as shown in Fig. 13. At the time of the beam hinge's failure, the externally applied load vector $\boldsymbol{R}^{\mathrm{Ext}}$ is modified to include the internal forces $\boldsymbol{R}_{\mathrm{b}}$ resulting from the failed beam end. The mass matrix $\boldsymbol{M}$ must also be modified because the beam mass $\boldsymbol{m}_{\mathrm{b}}$ at the failed joint is no longer assembled into the mass matrix for the structure. Its inertial effects are accounted for by use of the modified stiffness procedure described in the previous section. The

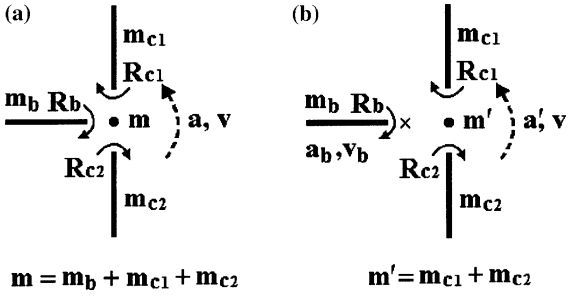


Fig. 13. Equilibrium of a node, (a) before fracture, (b) after fracture.

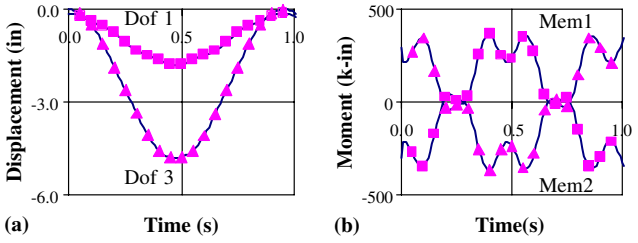


Fig. 12. Comparisons of computed results, (a) displacements for DOF 1 and 3, (b) bending moments of member 1 and 2 at Node 2.

tangent stiffness matrix $\boldsymbol{K}_t$ is also affected because of the loss of beam stiffness. Furthermore, the proportional damping matrix $\boldsymbol{C}$ needs to be updated using the modified $\boldsymbol{M}$ and $\boldsymbol{K}$ because Rayleigh damping has been assumed. These updating schemes physically represent the current state of the structural configuration. Note that, for this particular case, only one fracture is presented. Therefore, the updating is done only at the node connecting to the failed hinge. If several hinge failures occur, the same procedure is required at all nodes connecting to failed hinges.

After hinge failures occur, jumps in acceleration at the nodes connecting to the failed hinges will occur due to suddenly released forces. Displacements and velocities, however, retain the same values. These jumps in acceleration are also essential in satisfying equilibrium of the nodes. Considering the node shown in Fig. 13, the equilibrium equations just before and after fracture can be expressed as

$$\boldsymbol{ma} + \{\boldsymbol{R}_b + \boldsymbol{R}_{c1} + \boldsymbol{R}_{c2}\} = \boldsymbol{0} \tag{32}$$

$$\boldsymbol{m'a'} + \{\boldsymbol{R}_{c1} + \boldsymbol{R}_{c2}\} = \boldsymbol{0} \tag{33}$$

By adding and subtracting similar terms to both sides of Eq. (33), this equation can be rewritten as

$$\boldsymbol{m'}\{\boldsymbol{a} - \boldsymbol{m'}^{-1} \cdot (\boldsymbol{R}_{c1} + \boldsymbol{R}_{c2} + \boldsymbol{m'a})\} + \{\boldsymbol{R}_{c1} + \boldsymbol{R}_{c2}\} = \boldsymbol{0} \tag{34}$$

From Eq. (32), $\{\boldsymbol{R}_{c1} + \boldsymbol{R}_{c2} + \boldsymbol{m'a}\} = -\{\boldsymbol{R}_b + \boldsymbol{m}_b\boldsymbol{a}\}$. Thus, Eq. (34) can be expressed using the following expression

$$\boldsymbol{m'}\{\boldsymbol{a} + \boldsymbol{m'}^{-1} \cdot (\boldsymbol{R}_b + \boldsymbol{m}_b\boldsymbol{a})\} + \{\boldsymbol{R}_{c1} + \boldsymbol{R}_{c2}\} = \boldsymbol{0} \tag{35}$$

Eq. (35) indicates that the acceleration vector at the node under consideration changes abruptly by

$$\Delta\boldsymbol{a} = \boldsymbol{m'}^{-1} \cdot \{\boldsymbol{R}_b + \boldsymbol{m}_b\boldsymbol{a}\} \tag{36}$$

for which the resulting acceleration vector equals

$$\boldsymbol{a'} = \boldsymbol{a} + \Delta\boldsymbol{a} = -\boldsymbol{m'}^{-1} \cdot \{\boldsymbol{R}_{c1} + \boldsymbol{R}_{c2}\} \tag{37}$$

Therefore, at the onset of a beam hinge's failure, the current acceleration vector is updated according to Eq. (37).

## 4. Frame example

In this section, an example is given to demonstrate the importance of including dynamic effects for progressive collapse analysis. A two-bay, two-story frame with fixed supports (Fig. 14) has a uniform load of 0.4 kips/in acting on the beams. The first floor column on the right side of the building is assumed to fail abruptly by an abnormal load as indicated in Fig. 14(b). Following failure of the column, the remaining frame is analyzed from its original configuration using the developed computer program. Both static and dynamic analyses are performed, and the computed results are compared. In the current example, the damage parameters are set equal to zero so that a direct comparison can be made between the two analysis cases. For the dynamic analysis, the uniform load is applied as a rectangular pulse over the course of the analysis, and the time step size is set to be 0.005 s. A beam mass of 0.124 kips-s$^2$/in at each end is used for all members. In addition, rotational inertia and damping are ignored.

The results obtained from the static and dynamic analyses are summarized and compared through Figs. 15 and 16, and Table 1. The vertical displacement at Node $F$ is plotted versus time for both the elastic and inelastic analyses. For the static analysis, the maximum vertical displacement is equal to 2.65 in when elastic behavior is assumed, and it is 4.74 in when inelastic response is considered. For the dynamic analysis, the maximum vertical displacement obtained during the time history response is equal to 5.27 in for the elastic case (Fig. 15(a)), and equal to 14.51 in for the inelastic case (Fig. 15(b)). Fig. 16 shows plastic hinge locations obtained from the analyses. As can be seen from the figure, including inertial effects results in a response behavior with a greater number of plastic hinges. To assess the varying degrees of plasticity, plastic hinge rotations at points 1–4 (Fig. 16) are compared for the static and dynamic cases (Table 1).

In Table 1, dynamic increase factors (DIFs) are determined by computing the ratio of the maximum response for the dynamic case versus the static case. As can be seen from this table, the DIFs for the vertical displacements are equal to 1.99 and 3.06 for the elastic and inelastic cases, respectively. Furthermore, the DIFs for

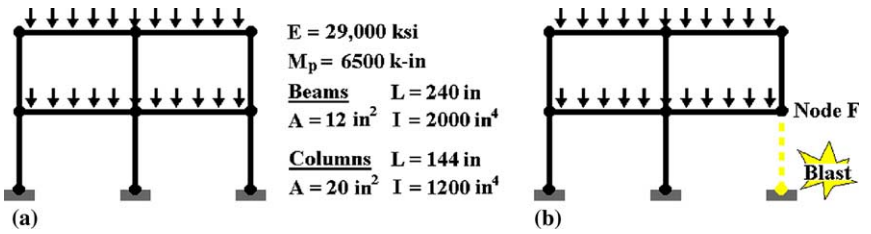


Fig. 14. Two-bay, two-story frame, (a) uniform load of 0.4 kips/in, (b) 1st floor column failure due to an abnormal load.

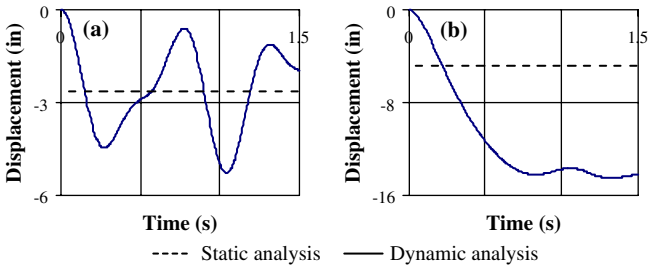


Fig. 15. Vertical displacements at Node $F$, (a) elastic analysis, (b) inelastic analysis.

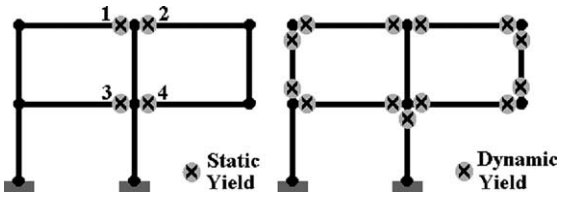


Fig. 16. Plastic hinges obtained from inelastic static and dynamic analyses.

Table 1
Comparison of analysis results

| | Static analysis | Dynamic analysis | DIF |
|---|---|---|---|
| Vertical disp. (elastic) (Node $F$) | 2.65 | 5.27 | 1.99 |
| Vertical disp. (inelastic) (Node $F$) | 4.74 | 14.51 | 3.06 |
| Plastic rotation (Point 1) | 0.007 | 0.023 | 3.29 |
| Plastic rotation (Point 2) | 0.008 | 0.034 | 4.25 |
| Plastic rotation (Point 3) | 0.003 | 0.017 | 5.67 |
| Plastic rotation (Point 4) | 0.012 | 0.038 | 3.17 |

the plastic rotations range from 3.17 to 5.67. In this example, the results demonstrate that accounting for dynamic effects of the response lead to greater inelastic deformations throughout the structure. Significantly, the extent to which plasticity spreads from the site of the original member failure is much greater for the case of the dynamic analysis in comparison to the static analysis.

## 5. Conclusions

Progressive collapse of buildings has been recognized as an important design consideration since the collapse of the Ronan Point Apartment building in 1968. Although a considerable amount of research related to progressive collapse has been reported, few researchers have addressed the importance of dynamic load redistribution following the sudden failure of one or more structural members. Results obtained in this research demonstrate that a static analysis may not provide conservative estimates of the collapse potential of frame structures. This issue is important given that most current design codes recommend the Alternate Load Path Method, a static-based approach, as a simplified analysis technique for determining whether or not a structure is likely to collapse following the failure of a key component.

In order to overcome the limitations of the Alternate Load Path Method, a framework for computing the dynamic response of frame structures during a progressive collapse event has been proposed. In this paper, a beam-column element formulation and solution procedure have been developed. The use of modified fixed-end forces and equivalent deformations has been employed to prevent violation of the yield function at member ends when member loads are present during the element state determination. A damage model has been introduced to account for both strength and stiffness degradation. This approach has the advantage that damage is computed explicitly so that the onset of member failure is determined in a rational manner. The rate of damage accumulation can be controlled through two parameters associated with the damage model. Perhaps the most significant feature of the computer program is the capability to continue an analysis after member failure has occurred. While many explicit finite element codes offer this capability, few implicit codes do. Therefore, the computational model developed for this research offers the advantages of numerical stability, computational efficiency because large time step sizes (relative to explicit codes) can be used, and the ability to compute the response of a structure after members have failed. To continue an analysis in an efficient manner after failure of a member, the solution scheme makes use of a modified member stiffness procedure so that no new nodes are introduced to the model. This approach has been effectively adapted from static condensation techniques to be used for dynamic analyses.

While the research presented in this paper demonstrates the essential aspects of dynamic progressive collapse analysis, it is important to point out that predicting progressive collapse behavior is a very com-

plex problem because the process is highly nonlinear, and it involves simultaneously the issues of member instability, damage evolution, ruptures of member joints, and impact forces of failed members. Most of these characteristics have not been conclusively identified in the literature, and little data exist to provide validation for computational models. Nevertheless, all of these issues are considered to be of great importance to the current research and have been included in the developed computer program. Some of these features have been addressed in an approximate way, and some have been addressed in a more detailed fashion. Future research will focus on conducting parametric studies to identify key factors that contribute to the progressive collapse of planar frame structures.

## References


[1] Breen JE. Research workshop on progressive collapse of building structures: Summary report. HUD-PDR-182, Department of Housing and Urban Development, 1976.

[2] Leyendecker EV, Ellingwood BR. Design methods for reducing the risk of progressive collapse in buildings: NBS Building Science Series 98, 1977.

[3] Hakuno M, Meguro K. Simulation of concrete-frame collapse due to dynamic loading. J Eng Mech 1993;119(9): 1709–23.

[4] Isobe D, Toi Y. Analysis of structurally discontinuous reinforced concrete building frames using the ASI technique. Comput Struct 2000;76(4):471–81.

[5] International Building Code. USA: International Code Council, 2000.

[6] DoD Interim Antiterrorism/Force Protection Construction Standards Progressive Collapse Design Guidance: Department of Defense, 2001.

[7] Progressive Collapse Analysis and Design Guidelines for New Federal Office Buildings and Major Modernization Projects: Central Office of the GSA, 2000.

[8] Pretlove AJ, Ramsden M, Atkins AG. Dynamic effects in progressive failure of structures. Int J Impact Eng 1991;11(4):539–46.

[9] Kaewkulchai G, Williamson EB. Dynamic progressive collapse of frame structures. The 15th Engineering Mechanics Division Conference, ASCE, New York, 2002.

[10] Malla RB, Nalluri B. Dynamic effects of member failure on response of truss-type space structures. J Spacecraft Rockets 1995;32(3):545–51.

[11] Malla RB, Nalluri B. Dynamic nonlinear member failure propagation in truss structures. Struct Eng Mech 2000; 9(2):111–26.

[12] Kim KD. Development of analytical models for earthquake analysis of steel moment frames. PhD Dissertation, The University of Texas at Austin, 1995.

[13] Park YJ, Ang AHS. Mechanistic seismic damage model for reinforced concrete. J Struct Eng 1985;111(4):722–39.

[14] Rao PS, Sarma BS, Lakshmanan N, Stangenberg F. Damage model for reinforced concrete elements under cyclic loading. ACI Mater J 1998;95(6):682–90.

[15] Krawinkler H, Zohrei M. Cumulative damage in steel structures subjected to earthquake ground motions. Comput Struct 1983;16(1–4):531–41.

[16] Ballio G, Castiglioni CA. Seismic behavior of steel sections. J Construct Steel Res 1994;29:21–54.

[17] Azevedo J, Calado L. Hysteretic behavior of steel members: Analytical models and experimental tests. J Construct Steel Res 1994;29:71–94.

[18] Williamson EB, Hjelmstad KD. Nonlinear dynamics of a harmonically excited inelastic inverted pendulum. J Eng Mech 2001;127(1):52–7.

[19] Cipollina A, Lopez-Inojosa A, Florez-Lopez J. A simplified damage mechanics approach to nonlinear analysis of frames. Comput Struct 1995;54(6):1113–26.

[20] Inglessis P et al. Model of damage for steel frame members. Eng Struct 1999;21(10):954–64.

[21] Baber TT, Wen YK. Random vibration hysteretic, degrading systems. J Eng Mech 1981;107(6):1069–87.

[22] Williamson EB. Evaluation of damage and $P$–$\Delta$ effects for systems under earthquake excitation. J Struct Eng-ASCE 2003;129(3):1036–46.

[23] Moehle JP, Elwood KJ, Sezen H. Gravity load collapse of building frames during earthquakes. Special Publication (SP-197) Uzumeri Symposium, American Concrete Institute, Farmington Hills, MI, 2002.

[24] Felton LP, Nelson RB. Matrix structural analysis. New York: Wiley; 1997.

[25] Newmark NM. A method of computation for structural dynamics. J Eng Mech 1959;85:67–94.

[26] Bathe KJ. Finite element procedures. New Jersey: Prentice-Hall; 1995.

[27] Belytschko T, Liu WK, Moran B. Finite elements for nonlinear continua and structures. New York: Wiley; 2000.

[28] Spacone E, Ciampi V, Filippou FC. Mixed formulation of nonlinear beam finite element. Comput Struct 1996;58(1): 71–83.

[29] Neuenhofer A, Filippou FC. Evaluation of nonlinear frame finite-element models. J Struct Eng 1997;123(7): 958–66.